2008 8th IEEE-RAS International Conference on Humanoid Robots
December 1 ~ 3, 2008 / Daejeon, Korea

Development of a New Wrist for the Next Generation of the Humanoid Robot ARMAR

Albert Albers[1], Jens Ottnad[1], Christian Sander[1]

[1] *University of Karlsruhe, IPEK - Institute of Product Development Karlsruhe, Germany,*
albers@ipek.uni-karlsruhe.de, ottnad@ipek.uni-karlsruhe.de, sander@ipek.uni-karlsruhe.de

***Abstract*— The development of a humanoid robot within the scope of the collaborative research centre 588 has the objective of creating a machine that can closely cooperate with humans. This development area presents new challenges for designers. In contrast to industrial robots – for which mechanical rigidity, precision and high velocities are primary requirements – the key aspects here are prevention of hazards to users, a motion space that corresponds to that of human beings, and a lightweight design. In order to meet these requirements, the robot must have humanlike appearance, motion space, and dexterity. Additionally, its kinematics should be familiar to the user, and its motions predictable, so as to encourage inexperienced persons to interact with the machine.**

This article gives insight into the design of a new wrist for the next generation of the humanoid robot ARMAR. The goals of the development project are both to improve the motion space and to achieve a humanlike appearance. The new mechanical design is described in detail completed by a study of a first prototype.

I. Introduction

The mechatronic design of a humanoid robot is fundamentally different from that of industrial robots. Industrial robots generally have to meet requirements such as mechanical stiffness, accuracy and high velocities. The key goal for this humanoid robot is not accuracy, but the ability to cooperate with humans. In order to enable a robot to interact with humans, high standards are set for sensors and control of its movements. The robot's kinematic properties and range of movements must be adjusted to humans and their environment [1].

A. The humanoid robot ARMAR

The collaborative research centre 588 "Humanoid Robots – learning and cooperating multi-modal robots" was established by the "Deutsche Forschungsgemeinschaft" (DFG) in Karlsruhe in May 2001. In this project, scientists from different academic fields develop concepts, methods, and concrete mechatronic components for a humanoid robot called ARMAR (see figure 1) that can share its working space with humans. The long-term target is the interactive work of robots and humans to jointly accomplish specified tasks.

For instance, a simple task like putting dishes into a dishwasher requires sophisticated skills in cognition and the manipulation of objects. Communication between robots and humans should be possible in different ways, including speech, touch, and gestures, thus allowing humans to interact with the robots easily and intuitively. As this is the main focus of the collaborative research centre, a humanoid upper body on a holonomic platform for locomotion has been developed. It is planned to increase the mobility of ARMAR by replacing the platform with legs within the next years, which will lead to modifications of the upper body.

Fig. 1 Upper body of the humanoid robot ARMAR III

B. State of the art and motivation

The focus of this paper is the design of a new wrist for the ARMAR robot. The wrist serves as the connection between forearm and hand; implementation of the new modules is planned for the next generations of the humanoid robot, ARMAR IV and V.

The wrist of the current version, ARMAR III, has two degrees of freedom [2] and its rotational axes intersect in one point. ARMAR III has the ability to move the wrist to the side (± 60°, radial/ulnar deviation) as well as up and down (± 30°, wrist flexion/extension). This was realized by a universal joint in a compact construction. The motors for both degrees of freedom are fixed at the support structure of the forearm. The gear ratio is obtained by a ball screw in conjunction with either a toothed belt or a cable. The load transmission is almost free from backlash. The angular measurement in the wrist is realized by encoders at the motors and with quasi-absolute angular sensors directly at the joint. To measure the load on the hand, a 6-axis force and torque sensor is fitted between the wrist and the hand.

One of the main points of criticism on the current version of the wrist is the offset between the rotational axes and the flange, as shown in figure 2. Due to the joint design, this offset distance is necessary in order to provide the desired range of motion. That offset is even greater due to the placement of the 6-axis force and torque sensor. The resulting

978-1-4244-2822-9/08/$25.00 ©2008 IEEE

movement, a circular path performed by the carpus, does not appear as a humanlike motion.

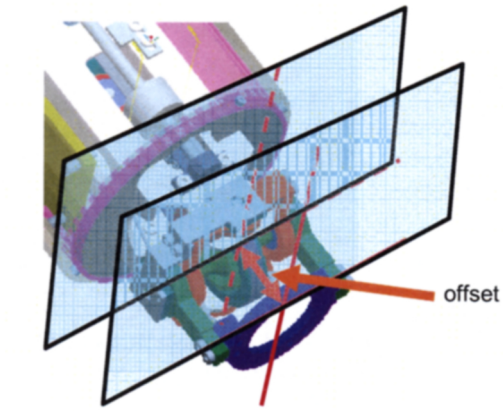

Fig. 2 Offset between the rotational axis and the hand flange at the wrist of the humanoid robot ARMAR III

The German Aerospace Centre DLR (Deutsches Zentrum für Luft- und Raumfahrt) has been working on seven degree of freedom robot arms for several years. Although their work is inspired by a human arm, their goal is not to design humanoid robots. The wrists of the lightweight arms of the third generation imitate human wrist movements by a pitch-pitch combination with intersecting axes (kardanic). An alternative pitch-roll configuration is also utilized, mainly for applications using tools [3]. Both versions have an offset comparable to the current wrist of ARMAR III.

Fig. 3 The DLR/Kuka lightweight robot arm [3]

In 1976 Henry J. Taylor and Philip N.P. Ibbotson designed a "Powered Wrist Joint" [4] in order to load and unload space shuttles. In a smaller version, the basic idea could be reused in humanoid robot's wrist. The second degree of freedom (pitch) of the wrist is guided by a spherical joint. Such an assembly provides a slim design and relatively wide range of motion. The actuators for the second degree of freedom (yaw) are located directly at the joint; therefore, the drive units are quite simple. On the other hand, miniaturization seems to be very difficult due to the dimensions of common gears and motors.

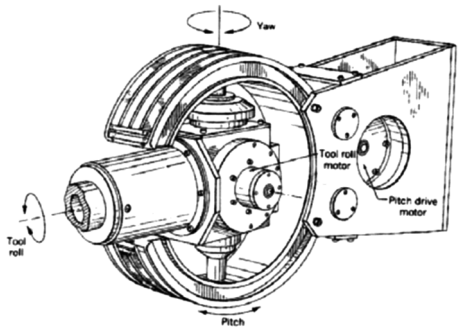

Fig. 4 Concept for a wrist actuator [4]

II. New Concept

C. *Requirements and design goals*

Since the robot will come in contact with humans in order to fulfill various functions, it is important that the robot is accepted by the human. The ability to move like a human is as important as a human-like appearance; therefore, specific demands [5] on kinematics, dynamics and the design space must to be considered.

A human wrist consists of many different elements and has a relatively wide range of motion. Figure 5 illustrates the different possible movements of the human wrist along with the corresponding reachable angular position of the joints.

In order to implement a human-like wrist movement, two orthogonally arranged rotational degrees of freedom are necessary. Both axes are orthogonal to the forearm's axis and intersect in one point. The two degrees of freedom need to be put in a kinematical series.

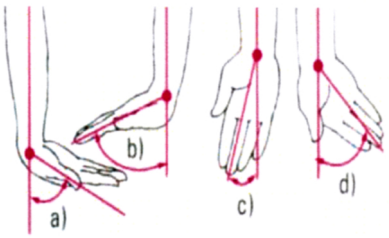

Fig. 5 Human wrist and range of motion: a = palmar flection 70°, b = dorsal flection 90°, c = radial abduction 20°, d = ulnar abduction 40° [6]

The requirements and design goals for a humanoid robot's wrist can be deduced based on the range of motion of the human wrist. The first degree of freedom should have a ±30° range of motion and the second ±90°.

The wrist will be attached to the forearm's structure on one side and provides the connection to the hand. It should be possible to disconnect the mechanical joint between the hand and wrist in a simple way in order to enable a modular design. To measure the load on the hand, a 6-axis force and torque sensor must be fitted between the wrist and the hand. The

electronic cables and pneumatic tubes supplying power to the hand actuators are the same as those used in the previous models of ARMAR [7,8].

The design space for the robot's wrist is based on human dimensions as much as possible; therefore, one aim is to keep a sphere of approximately 100 mm in diameter as a boundary. At the same time, the control strategy aims to operate all degrees of freedom as individually as possible.

In keeping with the standardized drive concept of most modules of the robot, electronic motors are used as the source for actuation. The drive units need to be dimensioned for a load of 3 kg. All gears are designed to be free from backlash and not self-locking. But friction, e.g. in case of a loss of power, leads to a slow and damped sinking of the arm instead of abrupt movement. That is of great importance for an interactive application of the robot in a human environment. On the other hand, stick-slip effects in the gears have been avoided, which is a clear benefit for the control system.

Finally, the mechanical structures should be as light as possible in order to save energy during dynamic movements. A lower mass of the wrist can contribute significantly to a reduced energy consumption of the whole arm and has a strong influence on the gears and motors used for the drive units for the elbow and shoulder degrees of freedom.

D. Concepts

A simple reduction of the wrist's length by only minor modifications is not possible. This is mainly because the current joint design in combination with the drive unit for the second degree of freedom does not allow a mounting of the hand in the rotational axis. Formulated in an abstract way, the development goal is to shift material from the intersection point to a different location in order to gain free space in the center position.

Bodies in general have six degrees of freedom in a three dimensional space: three rotational, and three translational. Due to design complexity, the degrees of freedom must be reduced for the development of a technical joint. As technical solutions in robotics usually have only one degree of freedom, it is necessary to combine two basic joints to implement a two degree of freedom joint. An alternative solution is a spherical joint where one rotation is blocked, but actuators for such a design have not yet been sufficiently developed.

As result of these basic considerations, two principle solutions were found: a universal joint and a kind of curved track as depicted in figure 6.

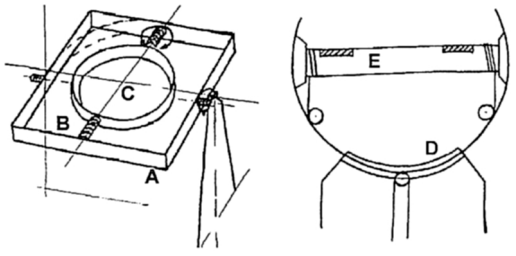

Fig. 6 Universal joint (left) and the principle curved track solution (right)

To illustrate the decision process within the development both concepts are discussed shortly. The universal joint concept (figure 6 left)is very similar to the current solution running on ARMAR III. The first degree of freedom is provided by rectangular frame (A). On that frame there is enough space for the bearings (B) of the second degree of freedom. Finally, the hand can be mounted on the plate (C). In contrast to the current version, the reduced length was achieved by taking all elements in one plane. The disadvantage is that the outer diameter had to be enlarged in order to provide the wide range of motion described in the previous section.

One possible implementation of the drive units could be a direct connection by Bowden cables providing a slim and light design of the joint itself. By applying this idea to the universal joint, the total length (TL) of each cable changes. Figure 7 illustrates the parameters which are of importance for a two dimensional consideration.

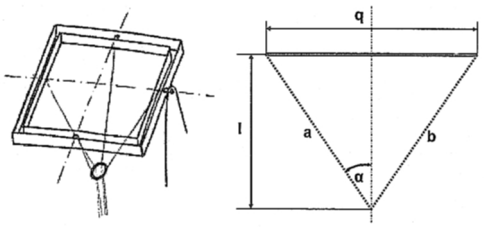

Fig. 7 "Changing" length of the cables in different angular positions of the wrist.

The TL can easily be calculated by the following formula, where α denotes the angle between the cables and the middle axis of the forearm:

$$TL = a + b = 2 \cdot \frac{l}{\cos(\alpha)} \tag{1}$$

As α depends on the angular position of the wrist, the TL changes during each movement. That means that the different degrees of freedom can not be run independently as long as electronic motors are used as actuators. The Shadow Hand, for example, uses a different concept concerning the cables and their changing lengths [10].

The second basic concept depicted in figure 6 on the right side consists of a curved track solution for the first degree of freedom (D). As this first rotation is limited to ±30°, there is enough space left for the bearings of the second degree of freedom, which may be realized, e.g., by a simple shaft (E). This configuration allows a relatively wide range of motion and a high capability for a reduction of the wrist's length. The challenges for this concept include finding a technical solution for the curved track and designing for the proper stiffness in the structures.

Overall, both basic concepts fulfill the principle requirement of length reduction. The curved track method, however, has a clear advantage in terms of size in the radial direction. The oval outer contour also shows a better similarity

to a human wrist; therefore, the curved track concept was selected for further development.

E. Embodiment design

By an appropriate design of the shaft (figure 6 right, named E) it is possible to gain still more space for the 6-axis force and torque sensor. Figure 8 illustrates a cross-section view of the modified shaft:

Fig. 8 Basic idea for the shaft of the second DOF of the wrist integrating the force sensor.

The depth of the shell corresponds with the radius of the curved track and enables a mounting of the hand exactly in the point where the rotational axes intersect. This is achieved by shifting the mechanical connection in the negative direction along the center axis of the forearm.

For the technical implementation of the curved track, a curved guide called. HCR manufactured by THK [9] was selected. Used for medical applications, THK produces ceramic curved guides with a radius of approximately 100mm. From a technical standpoint it would have been possible to reduce the radius to meet the requirements for a humanoid robot's wrist. For economic reasons, however, this was not a feasible option for the collaborative research centre. Therefore, a different solution was necessary.

The curved guide was replaced by rollers in combination with a timing belt. This allowed for the integration of two different functions in one element: the timing belt functions as part of the drive unit while also providing sufficient pre-load to avoid a gap between the rollers and the track. Figure 9 shows the basic CAD model of each design.

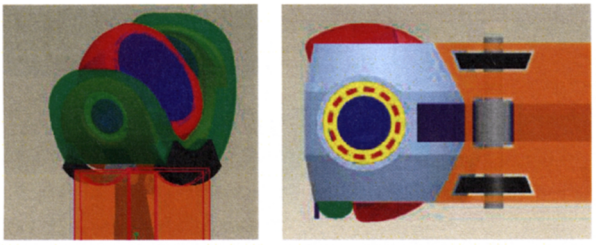

Fig. 9 First technical solution by using a curved guide (left) and the alternative using a roll timing belt combination (right)

To investigate the new concept, different analyses and simulations were conducted and are described in the next chapter.

III. Simulation

A. Basic geometric considerations

Based on the new concept introduced and explained in Chapter II, an analytic model can be created. Therefore all geometrical parameters based on the nature of the human body have to be adapted to the model. The undefined variables have to be calculated and estimated using the analytical model to get a reasonable collection of values for the design. Using parameter optimization the best combination of values for a design proposal can be found in order to achieve reasonable preloads for the belt. Thus forces and moments are been calculated. To reduce the complexity of the calculation and to get a rough estimate the consideration of a static model is sufficient. The primary objective of the analytical method is to get an estimated range of the needed preloads for the timing belt to ensure the stability of the mechanical system. Thereupon a decision can be made if a numeric simulation using the finite element method (FEM) could be useful or even necessary.

The system has two main load cases whereas the angle of the initiated force φ can vary. Figure 10 illustrates these two load cases. Here the external force F_2 given by the list of requirements and the internal forces F_0 and F_1 resulting from the self-weight (gravitational vector points at the direction of the external force). To avoid a displacement of the cap the preload $F_{V,3}$ has to be chosen great enough. The force $F_{V,2}$ results from an axial displacement q shown in figure 11.

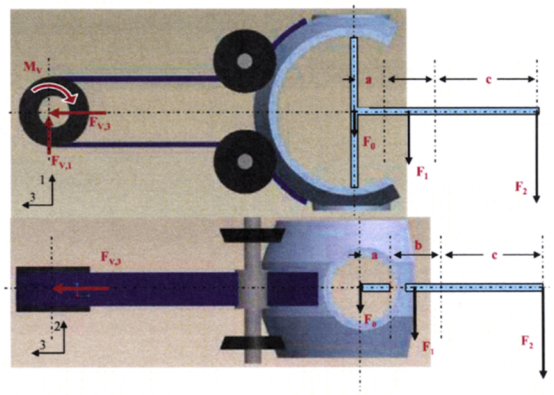

Fig. 10 Load case I (upper) and load case II (lower) in two different directions

In order to start the analysis all relevant geometrical constants have to be defined and collected. Furthermore all variables have to be identified. The force F_{ers} was defined as substitute for the forces F_0, F_1 and F_2 and its point of application is at F_0 in the center of the second DOF. Its absolute value is 36 N. Resulting from the arm of lever an additional torque have to be added to the substituted force F_{ers}. It's named M_{ers} and it averages about 3,14 Nm. Using the equilibrium conditions given by the technical mechanics and provided that the system is static, the resulting forces and torques can be calculated. Herewith the searched minimal preload of the timing belt has been found.

1) Load case I:

From the schematic drawing in figure 11 showing the first load case of the wrist, all relevant geometrical parameters are identified. The corresponding values are listed in Table 1.

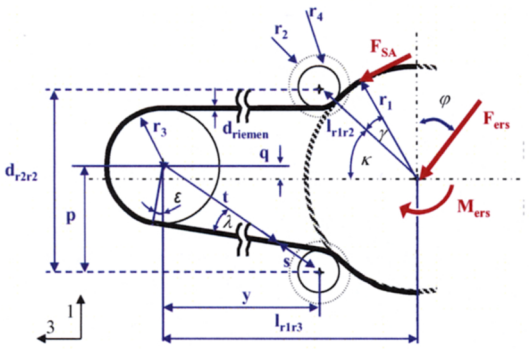

Fig. 11 Geometrical parameters of load case I

TABLE I
VARIABLES AND CORRESPONDING VALUES FOR ANALYTICAL CALCULATIONS

Variable	Value		Constant	Value
d_{r2r2}	<100 [mm]		l_{r1r3}	100 [mm]
y	$<l_{r1r3}$		r_1	40 [mm]
r_2	$>r_4$		r_3	10 [mm]
φ	±90°		r_4	4 [mm]

Using the defined values and trigonometric functions, the missing angles and variables depending on d_{r2r2} and r_2 can be calculated. At this point another additional variable has to be introduced. The direction of the external load has a variable angle towards the vertical line (figure 11) and is labeled φ. Figure 12 shows the preload of the timing belt against the angle of the load for two different graphs of various settings of d_{r2r2} and r_2.

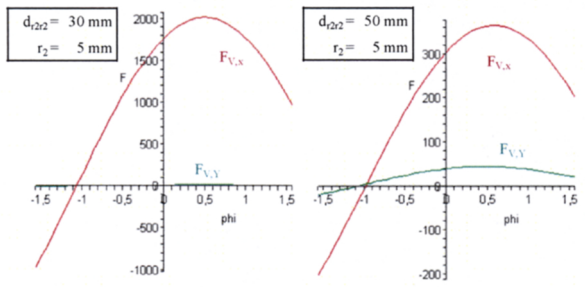

Fig. 12 Preload against φ [rad] for d_{r2r2}=30 mm, r_2=5 mm (left) and d_{r2r2}=50 mm, r_2=5 mm (right)

The required preload for an offset of the bevel wheels of 37,5 mm is about 1000 N. When d_{r2r2} is 42,5 mm, the required force is less than 631 N. Thus, the required force decreases by about 37 % when the offset of the beveled wheels is increased by about 21 %. When this distance is doubled from 35 mm to 70 mm, the required preload force is reduced by 90 %. The critical angle of the load, φ, is 36°.

2) Load case II

A schematic drawing of the second load case can be seen in figure 13. Calculations have disclosed that the influence of the substituted shear force F_{ers} is negligible; therefore, only the over-all torque M_{ers} is used for the analysis.

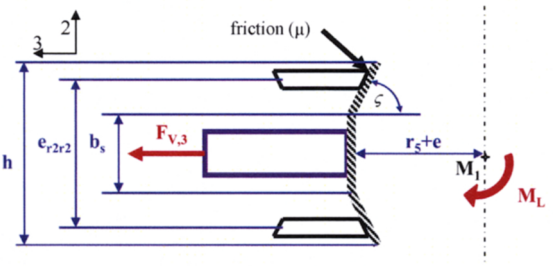

Fig. 13 Geometrical parameters of load case II (only shear force)

The height h, the width b, the radius r_5, the friction μ and the distance e to avoid unwanted contact between belt and structure are given. Therefore the preload force $F_{V,3}$ is dependent upon the angle ς and the wheel distance e_{r2r2}. In figure 14 the preload force is plotted. The maximum force for the timing belt is 280 N. And while increasing the angle ς and increasing the offset of the bevel wheels e_{r2r2} from the maximum the preload force decreases.

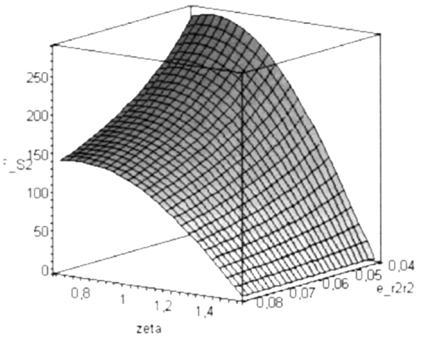

Fig. 14 Preload against er2r2 and ς with μ=0,3

The calculated forces are all reasonable and can be realized in a real system with standard bearings and materials. Up to this point there is nothing to be said against this solution.

B. Design using the analytical results

On the basis of the analytic results described in section A, the optimal solution for the free geometrical parameters can be defined and in a further step be designed in a CAD environment. A picture of the parameter optimized wrist is provided in figure 15.

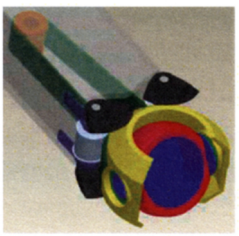

Fig. 15 Parameter optimized wrist

This CAD model is been discretized and numerically simulated using the finite element method. The preload force and the orientation of the external force were varied systematically. The primary object is to get values for the displacement of the cap towards the global coordinate system. ABAQUS (Dassault Systèmes) is the used solver for the FEM. In order to reduce the computing time, the CAD model must be simplified while the fundamental behavior of the system should be modeled as accurately as possible. Following parts are been simulated. The cap, the bevel wheels, the idler and the timing belt are modeled as deformable with the ABAQUS element type "C3D8I" (except bevel wheels, C3D8R). Analytical rigid elements are used for the connecting wheels and the driving shaft. All deformable parts are simulated with an isotropic material characteristic except for the timing belt. Because the timing belt is composed of a steel cord with polyurethane backing and teeth, an anisotropic material parameter is used in the model. Fortunately, the belt is symmetric about the "3" axis that is normal to a plane of isotropy (figure 16) and within this type of material, the number of independent constants in the elastic tensor are reduced to 5 from a total of 21 independent constants in case of fully anisotropy. This type of material is called transverse isotropy. But unfortunately none of the required parameters are documented by the producers. For that reason the elastic modulus and the Poisson's number have to be estimated.

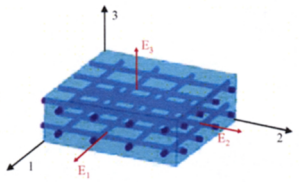

Fig. 16 Transverse Isotropy

The material constants for the simulation are summarized in Table 2 [11].

TABLE II
MATERIAL PARAMETERS

Material	E-Modulus $[\frac{N}{mm^2}]$	Poission's number	Zugeordnete Körper
Steel	210 000	0,30	Umlenkrolle
Aluminum	72 000	0,34	Handgelenksschale, Kegelräder
Belt material	$E_1=E_2=50\,000$, $E_3=5000$	$\nu_{12}=\nu_{13}13=0,33$ $\nu_{23}=0,44$	Toothed belt

The direction of the external load is as shown in figure 11 and 13 of the analytic analysis. However, the load vector alternates at each step of the timing belt's preload force. The angle φ of the external load takes the value of 0° and 36° which is identified in the analytic calculation as the most critical. Figure 17 illustrates the graphical result of the FEM simulation. The load is distributed reasonably.

Fig. 17 Stress distribution (von Mises) for load case II

The displacement of the cap under high preload forces is minimal due to the FEA. For a preload of 1000 N the displacement for the second load case is about $4{,}07 \cdot 10^{-3}$ mm and for load case I its value takes $1{,}29 \cdot 10^{-2}$ mm. The displacement of load case I with φ=36° is for every point smallest compared with load case I (φ=0°) and load case II. Therefore this load case will not be addressed any further. The absolute value of the displacement diversify minimal in the rage between F_V=600 N and 1000 N. The high additional costs in the construction of the wrist for preloads lager than 600 N would only result in a small increase of positioning accuracy. For this reason, and for practical implementation, it is not meaningful to use forces greater than 600 N. For preloads lower than 250 N the position deviation increases dramatically and the system becomes statically indeterminate.

Therefore, it appears that a preload between 250 N and 600 N would be most suitable.

C. Lightweight design by topology optimization

1) Methodology

Topology optimization is used for the determination of the basic layout of a new design. It involves the determination of features such as the number, location and shape of holes, and the connectivity of the domain. A new design is determined based upon the design space available, the loads, possible bearings, and materials of which the component is to be composed. Today topology optimization is very well theoretically studied [7] and also a very common tool in the industrial design process [8]. The designs obtained using topology optimization are considered design proposals. These topology optimized designs can often be rather different compared to designs obtained with a trial and error design process or designs obtained from improvements of existing layouts. The standard formulation in topology optimization is often to minimize the compliance corresponding to maximize the stiffness using a mass constraint for a given amount of material. That means that for a predefined amount of mass the structure with the highest stiffness is determined. Compliance optimization is based upon static structural analyses, modal analyses or even non-linear problems, such as models including contacts. A topology optimization scheme is

basically an iterative process that integrates a finite element solver and an optimization module.

Based on a design response supplied by the FE solver (e.g. strain energy), the topology optimization module modifies the FE model.

2) Model Setup

For the topology optimization the complete system is disassembled and only the cap with the connecting wheel, still a rigid body element, is used for the simulation. This simplification is necessary to avoid enormous computing time caused by a very fine mesh for the cap and a huge number of load cases. Cutting these two parts free from the total system, calls for a realistic replacement of the interactions between the components. Hereby the interaction between the bevel wheels and cap is replaced by a fixed connection at the corresponding nodes. This simplification is possible because the appearing forces can only be compressive forces. The timing belt is replaced by a line load which is tangential to the cap. The preload used in place of the timing belt is 450 N and is transferred by the line load. The external load is 36 N and the torque represents 3.1 Nm. The torque is applied rotates about the 3-axis and the force vector is parallel to the 1- and 2-axis (see figure 10). The algebraic sign of the force and the torque alternates to prevent one-sided undesired effects. Another load case is defined for the angle φ=36° of the external load. These five load case combinations are set for three different rotational positions of the second DOF. The initial state is the neutral position and two other positions are realized by changing the direction and position of all forces on the cap as they would appear at a ±30°rotation. From this it follows that 15 different configurations of the cap are set for the topology optimization.

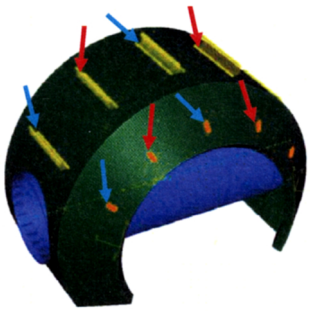

Fig. 18 FE model for topology optimization

In figure 18 the initial position at 0° is highlighted with red arrows and for a rotation of 30° with blue arrows (hidden forces and fixed connections are not highlighted).

3) Results

The design proposal as a result of the topology optimization is shown in figure 19. The mass is reduced by approximately 45% of the original design space. For a final design the components (e.g. the bearing carriers) need to be modified and adapted to a certain manufacturing process. The final mass and structure of that part will of course depend also on the used materials but the optimization results can give a first design proposal.

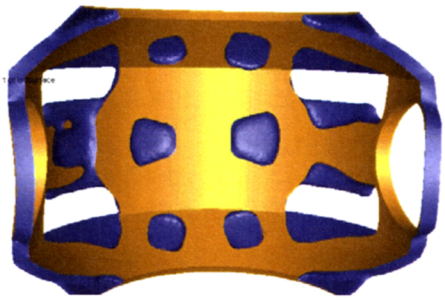

Fig. 19 Design proposal as result of the topology optimization for a lightweight design

On the basis of the design proposals obtained from the topology optimization a CAD model is implemented. In figure 20 the four holes can be seen. The running surface for the bevel wheels is also shortened in order to provide enough space for the required ±30° rotation angle. However, the wall for the bearings is thickened in order to provide more stability. The ripping in the contour is not adopted because the weight reduction compared to the additional work is disproportionate.

Fig. 20 Final design of the Cap

IV. FUNCTIONAL PROTOTYPE

Based on the positive results obtained by the different simulations, a functional prototype was developed. That was necessary mainly because different functions were integrated in the toothed belt, which is usually used in a different manner.

As the job of the prototype is to prove the functionality of the design, a few simplifications are made. The bevel wheels have a complete circle of 360° and the cap does not have the holes from the topology optimization. Furthermore, the construction allows the possibility to implement an s-beam force sensor (Lorenz K-25). Figure 21 shows a picture of the assembled, functional prototype with a one kilogram weight attached.

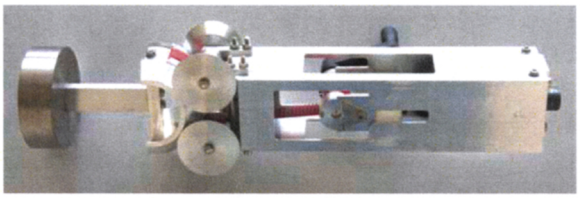

Fig. 21 Functional prototype

Multiple static and dynamic tests show that this configuration is very accurate and has a high stiffness for small preloads of about 300 N. Hereby the wrist is hand held at the forearm tube and statically loaded by huge forces between 20-80 N or moved dynamically in all different directions. Even for very "hand actuated" fast motions, which were approximately than five times the maximum velocity of the robot arm, the assembly remained free from backlash.

V. Conclusions

In this paper a new concept for humanoid robot's wrist is presented. Especially the different steps of the development process are described. Based on the basic ideas, different analyses and simulations are conducted. Due to the design proposal obtained by the topology optimization, a lightweight design is implemented in the CAD model. Finally, a functional prototype is presented which is a kind of proof of concept.

The next step will be the integration of the drive units for the second degree of freedom. Here different solutions are possible, e.g. like Bowden Cables or a direct actuation in combination with harmonic drive gears. The sensors for position and velocity measurement can be used in a manner similar to the current version ARMAR III [2]. In order to achieve a further reduction in mass, composite materials may be used for some of the structural components. The new wrist will be developed in the next months and is to be manufactured and assembled during the next year.

Acknowledgment

The work presented in this article is funded by the "Deutsche Forschungsgemeinschaft" (DFG) within the Collaborative Research Centre 588 "Humanoid Robots - Learning and Cooperating Multimodal Robots".

References

[1] C. Schäfer: Entwurf eines anthropomorphen Roboterarms: Kinematik, Arbeitsraumanalyse, Softwaremodellierung, Dissertation Fakultät für Informatik, Universität Karlsruhe, 2000.

[2] Albers A., Brudniok S., Ottnad J., Sauter Ch., Sedchaicharn K.: Upper Body of a new Humanoid Robot – the Design of armar III, Humanoids 06 - 2006 IEEE-RAS International Conference on Humanoid Robots, December 4 to 6, 2006 in Genova, Italy

[3] A. Albu-Schäffer, S. Haddadin, Ch. Ott, A. Stemmer, T. Wimböck, G. Hirzinger: The DLR lightweight robot: design and control concepts for robots in human environments, Industrial Robot: An International Journal, Vol. 34 No. 5, 2007

[4] M. Rosheim: Robot wrist actuators, 1. Auflage, 1989 ISBN 0-471-61595-1

[5] T. Asfour: Sensomotorische Bewegungskoordination zur Handlungsausführung eines humanoiden Roboters, Dissertation Fakultät für Informatik, Universität Karlsruhe, 2003.

[6] Wirhed: Sportanatomie und Bewegungslehre, Schattauer Verlag, 3. Auflage

[7] S. Beck, A. Lehmann, Th. Lotz, J. Martin, R. Keppler, R. Mikut: *Model-based adaptive control of a fluidic actuated robotic hand*, Proc., GMA-Kongress 2003, VDI-Berichte 1756, S. 65-72; 2003.

[8] S. Schulz: Eine neue Adaptiv-Hand-Prothese auf der Basis flexibler Fluidaktoren, Dissertation, Fakultät für Maschinenbau, Universität Karlsruhe (TH), 2003

[9] THK: www.thk.com

[10] www.shadow.org.uk: The Shadow Robot Company

[11] Paland, Prof. Dr.-Ing, Technisches Taschenbuch, 7. Ausgabe, INA 2002

[12] Bendsoe, M.; Sigmund, O.: Topology Optimization – Theory, Methods, Application, Springer Verlag 2003

[13] Pedersen, C.B.W.; Allinger, P.: Recent Developments in the Commercial Implementation of Topology Optimization. TopoptSYMP2005 - IUTAM-Symposium- Topological design optimization of structures, machines and material – status and perspectives. Copenhagen, Denmark, 123-132, 2005